Effect of temperature, pressure and chemical composition on the electrical conductivity of granulite and geophysical implications

Wenqing SUN**, Lidong DAI*, Heping LI*, Haiying HU* and Changcai LIU**

*Key Laboratory of High-Temperature and High-Pressure Study of the Earth's Interior, Institute of Geochemistry, Chinese Academy of Sciences, Guiyang 550081, China
**University of Chinese Academy of Sciences, Beijing 100049, China

Electrical conductivities of three granulite samples (main minerals: plagioclase, quartz, and biotite) with different chemical compositions (W_B, the weight percent of Fe_2O_3 = 5.49, 8.75, and 14.79 wt%) were researched using a complex impedance spectroscopic technique at 1.0–3.0 GPa and 623–1073 K from 10^{-1} to 10^6 Hz. The experimental results indicated that the granulite conductivities markedly increased with temperature and slightly decreased with increasing pressure. Under the experimental conditions, the temperature dependence of the conductivities of granulite followed an Arrhenius relationship at certain temperatures. The electrical conductivities of granulite significantly increased with increasing biotite content and W_B. According to the activation enthalpies and previous studies, the conduction mechanism of the granulite samples with W_B = 8.75 and 14.79 wt% was small polaron conduction under the experimental conditions, and the conduction mechanisms of the granulite sample with W_B = 5.49 wt% were small polaron conduction at high temperatures and impurity conduction at low temperatures. The high conductivity anomalies under the ductile shear zones in southern India can be interpreted by the conductivities of granulite with interconnected biotite and a high iron content (>14.79 wt%).

Keywords: Electrical conductivity, Granulite, High pressure, Conduction mechanism, High conductivity anomaly

INTRODUCTION

The material composition and thermodynamic state in the earth's interior can be inferred by combining the electrical conductivities of minerals and rocks with magnetotelluric (MT) and geomagnetic depth sounding (GDS) results. Previous studies have investigated the electrical conductivities of most minerals and rocks in the crust and upper mantle (Xu et al., 2000; Wang et al., 2010; Zhou et al., 2011; Yang et al., 2012; Hu et al., 2013; Dai and Karato, 2014; Dai et al., 2014; Hu et al., 2014; Podoba et al., 2014; Hui et al., 2015; Manthilake et al., 2015; Dai et al., 2016; Li et al., 2016; Manthilake et al., 2016; Hu et al., 2017; Li et al., 2017; Romo et al., 2017; Chen et al., 2018; Dai et al., 2018; Hu et al., 2018). However, the electrical conductivities of granulites with various chemical compositions at high temperatures and pressures have not been studied in detail. To research the electrical structure, material compositions, and thermodynamic state in the Earth's interior, it is necessary to investigate the electrical conductivity of granulites with various chemical compositions.

Granulite is formed by the high-grade metamorphism of protolith at the depth of the middle–lower crust. As an important metamorphic rock, granulite is distributed in some regional metamorphic belts (Zhang et al., 2004; Patro et al., 2014; Takamura et al., 2016; Wu et al., 2016). Southern Granulite Terrane (SGT), which is the high-grade metamorphic terrane of southern India, was formed during Ediacaran–Cambrian metamorphism and deformation and is comprised of four main tectonic units: the Salem Block, the Madurai Block, the Trivandrum Block, and the Nagercoil Block. Regional metamorphic rocks (such as schist, gneiss, granulite, and eclogite) are widely distributed in SGT (Collins et al., 2014). Electrical properties of some metamorphic rocks at high temperature and high pressure have been researched by previous studies. Mathez et al. (1995) researched the electrical conductivity of a water-saturated quartz-mica-

doi:10.2465/jmps.181107b
L. Dai, dailidong@vip.gyig.ac.cn Corresponding author

garnet-schist at atmospheric temperature and up to 200 MPa. It was found that the schist conductivity increases with increasing pressure. Fuji-ta et al. (2007) investigated the electrical conductivity of gneiss at 1.0 GPa and up to 1000 K, and the conductivity of gneiss perpendicular to the foliation can account for the subsurface conductivity structure beneath central Kyushu, Japan. To explore the influence of chemical compositions on the electrical conductivity of gneiss, Dai et al. (2018) measured the conductivity of gneiss with various chemical compositions at 0.5-2.0 GPa and 623-1073 K and found that the gneiss conductivity significantly increased with an increase in the alkali and calcium ion contents. However, the conductivity of gneiss with various chemical compositions cannot be used to interpret the high-conductivity anomalies under the Dabie-Sulu ultrahigh-pressure metamorphic belt. Dai et al. (2016) carried out electrical conductivity measurements for dry eclogite at 1.0-3.0 GPa, 873-1173 K and with three solid-state oxygen buffers (Cu + CuO, Ni + NiO, and Mo + MoO_2). However, the conductivity of eclogite cannot explain the high-conductivity layers (HCLs) under the stable middle-lower crust and the Dabie-Sulu ultrahigh-pressure metamorphic belt of eastern China. Fuji-ta et al. (2004) studied the electrical conductivity of granulite at 1.0 GPa and 300-890 K, and the experimental results can account for the conductivity structure in the mid- to lower crust of Hidaka metamorphic belt (HMB) in Hokkaido of Japan. However, the effect of pressure and chemical compositions on the electrical conductivity of granulite has not been researched, and the conduction mechanism for granulite is still unclear.

In this study, the electrical conductivities of granulite samples were measured at 1.0-3.0 GPa and 623-1073 K. The effects of temperature, pressure, and chemical composition on the granulite conductivities have been discussed in detail. According to the activation enthalpies and dependence of electrical conductivities on the chemical composition, we proposed conduction mechanisms for the granulite samples. Furthermore, we explored the geophysical implications of our findings for the high-conductivity anomalies observed under southern India.

EXPERIMENTAL PROCEDURES

Sample Preparation

Three granulite samples were collected from a rock mass in Altai, Xinjiang, China. The distribution of main minerals in the granulite samples was relatively homogeneous, and the sample surfaces were fresh, unoxidized, and unfractured. The mineralogical assemblage of the granulite samples was determined by optical microscopy and scanning electron microscopy at the State Key Laboratory of Ore Deposit Geochemistry, Institute of Geochemistry (SKLODG), Chinese Academy of Sciences (CAS), Guiyang, China. X-ray fluorescence spectroscopy was used to determine the chemical compositions of the granulite samples at the Australian Laboratory Services, Shanghai, China. As shown in Figure 1 and Table 1, the main rock-forming minerals of the granulite samples were feldspar, quartz, and biotite, and biotites in the samples remained oriented and interconnected to some extent. The contents of the major elements in the granulite samples varied (Table 2).

To determine the distribution of water in the granulite samples, the infrared spectra of biotite, quartz, and plagioclase in DS17 before and after electrical conductivity measurements were collected using a Fourier transform vacuum infrared spectrometer (Vertex 70V and Hyperion-1000 infrared microscope) at the Key Laboratory of High-Temperature and High-Pressure Study of the Earth's Interior, Institute of Geochemistry (KLHTHPSEI), CAS, China. Samples were polished to be 80-μm thick slices. The IR absorption of samples was measured by unpolarized radiation with a tungsten light source, a CaF_2 beam splitter, and an MCT detector with a 100 μm × 100 μm aperture. Spectra were collected in the wavenumber range of 3000-4000 cm^{-1} with 512 scans accumulated for per sample. As shown in Figure 2, the IR absorbance of biotite was much higher than that of feldspar and quartz before and after dehydration.

Impedance Measurements

Electrical conductivity measurements were carried out in a YJ-3000t multi-anvil apparatus and Solartron-1260 impedance/gain-phase analyzer at KLHTHPSEI, CAS, China. Figure 3 shows a schematic of the cross section of the experimental assemblage for electrical conductivity measurements of the granulite samples at high temperatures and pressures. To avoid the influence of free water on the electrical conductivity measurements, all components of the sample assembly (pyrophyllite, ceramic tubes, and Al_2O_3 and MgO sleeves) were baked at 1073 K in a muffle furnace for 12 h before the electrical conductivity measurements. Natural granulite samples were cut and polished into cylinders with diameter and height of 6 mm, and these were ultrasonically cleaned using a mixture of deionized water, acetone, and ethanol. The cylindrical samples were heated at 473 K for 8 h in an oven to remove absorbed water before subsequent measurements. In the sample assembly, a pyrophyllite cube (32.5 × 32.5 × 32.5 mm^3) and three-layer stainless-steel sheets (total thickness: 0.5 mm) were used as the pressure medium

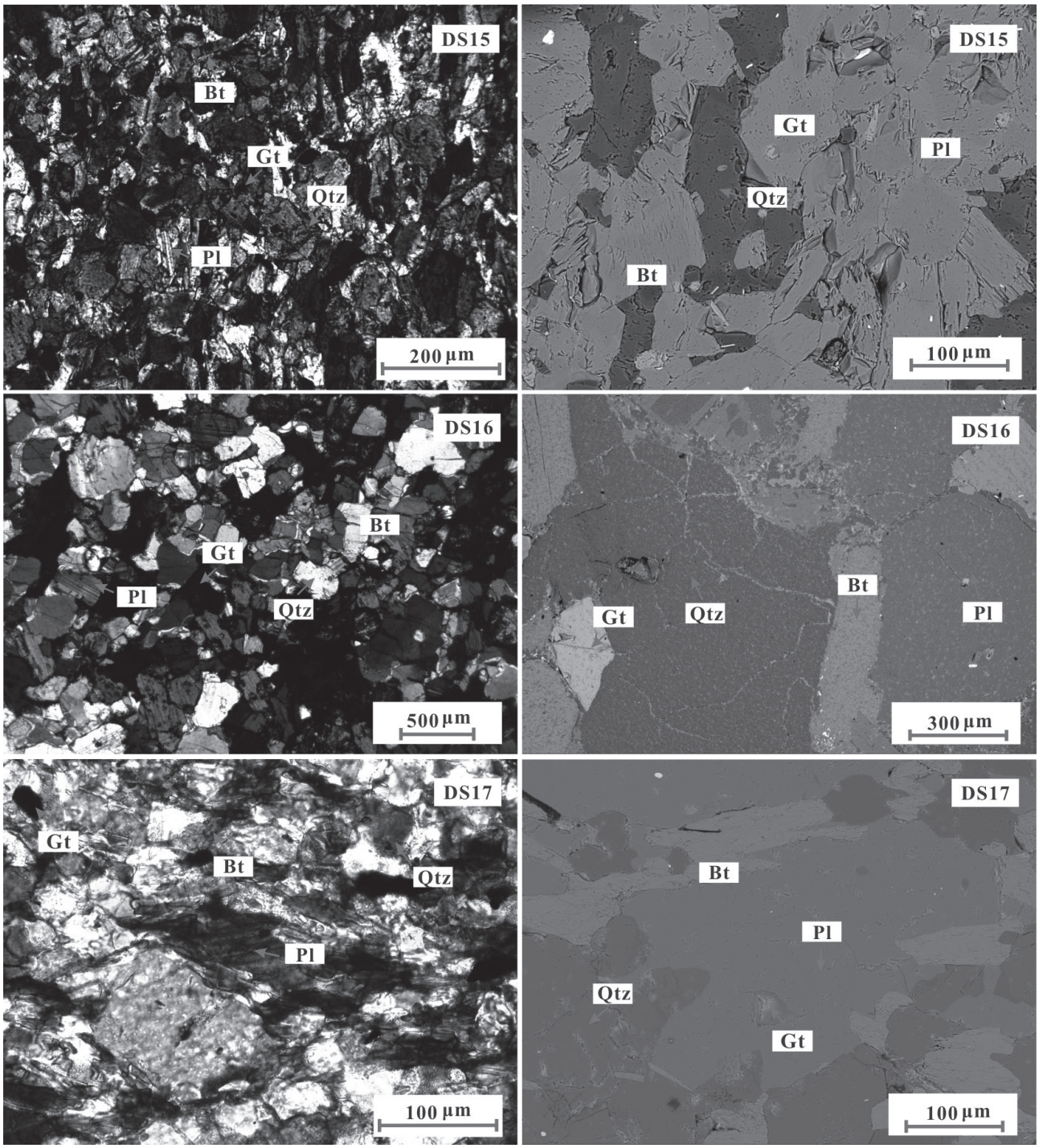

Figure 1. Photomicrographs and electron backscattered images of three natural granulite samples. Pl, plagioclase; Qtz, quartz; Bt, biotite; Gt, garnet. Color version is available online from https://doi.org/10.2465/jmps.181107b.

and heater, respectively. Alumina and magnesia sleeves as insulators were located between the heater and sample. To shield against external electromagnetism and spurious signal interference, a sheet of nickel foil (thickness: 0.025 mm) was installed between the alumina and magnesia sleeves. The sample was loaded into the magnesia tube, and then two nickel disks (diameter: 6.0 mm and thickness: 0.5 mm) were placed on the top and bottom of the sample as electrodes. The nickel electrodes and nickel foil can control the oxygen fugacity of the sample chamber (Dai et al., 2009; Faul et al., 2018). Before the electrical conductivity measurements, the sample assembly

Table 1. Mineralogical assemblage of three natural granulite samples

Run	Mineral associations
DS15	Pl (40%) + Qz (28%) + Bi (30%) + Gt (2%)
DS16	Pl (30%) + Qz (45%) + Bi (20%) + Gt (5%)
DS17	Pl (50%) + Qz (35%) + Bi (13%) + Gt (2%)

Pl, plagioclase; Qz, quartz; Bi, Biotite; G, Garnet.

Table 2. Chemical composition of whole rock analysis by X-ray fluorescence (XRF) for three granulite samples

Oxides (wt%)	DS15	DS16	DS17
SiO_2	44.16	58.74	63.31
Al_2O_3	18.34	18.80	15.78
MgO	5.76	4.37	2.82
CaO	10.90	1.79	1.68
Na_2O	2.43	1.96	3.31
K_2O	0.38	2.89	5.24
Fe_2O_3	14.79	8.75	5.49
TiO_2	1.93	0.90	0.62
Cr_2O_3	<0.01	0.02	0.01
MnO	0.24	0.10	0.06
BaO	0.02	0.06	0.06
SrO	0.04	0.02	0.02
P_2O_5	0.36	0.14	0.14
SO_3	0.02	<0.01	<0.01
L.O.I	0.96	1.30	1.01
Total	100.33	99.84	99.55

was placed in an oven at 323 K to avoid the effect of moisture.

During the experiments, the pressure was increased slowly at 1.0 GPa/h until it reached the desired value, and then the temperature was increased at 600 K/h to the designated value. The impedance spectra of the samples at an applied voltage of 1 V were collected in the frequency range of 10^{-1}–10^{6} Hz when the designated pressure and temperature were stable. At the desired pressure, the impedance spectra were measured in multiple heating/cooling cycles until reproducible data were obtained, and the measured temperature interval was 50 K. To study the influence of pressure on the granulite conductivities, the conductivities of the granulite sample DS17 were measured at 1.0–3.0 GPa and 623–1073 K. The conductivities of the granulite samples of DS15 and DS16 were measured at 2.0 GPa and 623–1073 K. The errors of temperature and pressure were ±5 K and ±0.1 GPa, respectively.

RESULTS

Representative complex impedance spectra of the granulite samples are shown in Figure 4. The spectra were composed of an almost ideal semicircle in the high-frequency region and an additional tail in the low-frequency region. Previous studies have proposed that the ideal semicircle in the high-frequency region represents the bulk electrical properties of the sample, and the additional tail is related to diffusion processes at the sample-electrode interface (Roberts and Tyburczy, 1991; Saltas et al., 2013). Therefore, the bulk sample resistance can be obtained by fitting the ideal semicircle in the high-frequency region. A series connection of R_S-CPE_S (R_S and CPE_S represent the resistance and constant-phase element of the sample, respectively) and R_E-CPE_E (R_E and CPE_E represent the interaction of charge carriers with the electrode, respectively) was used as the equivalent circuit, and the fitting errors of the electrical resistance were less than 5%. Based on the sample size and electrical resistance, the electrical conductivity of each sample was calculated according to:

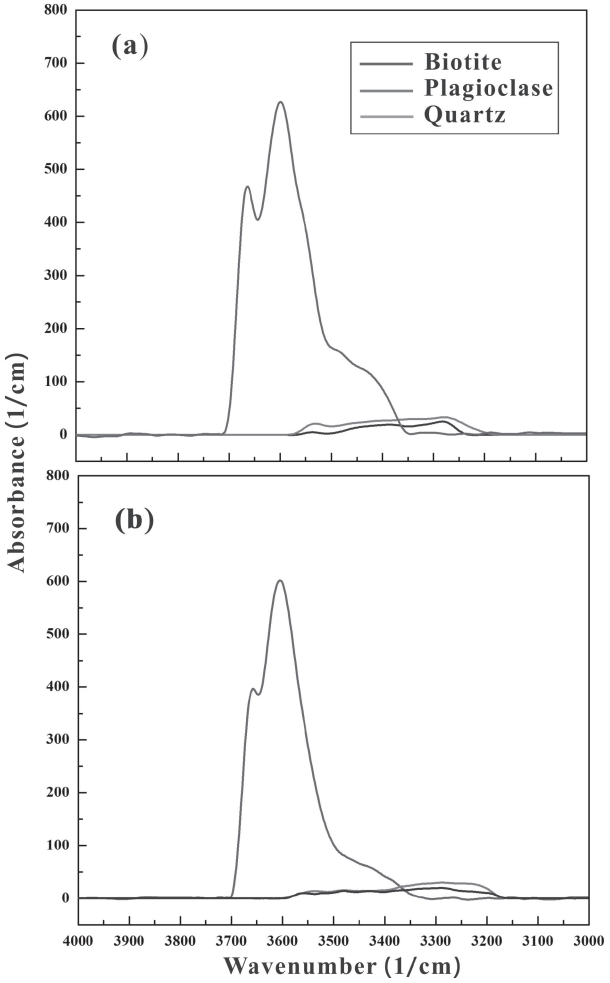

Figure 2. The representative FT-IR spectra of biotite, plagioclase and quartz in the granulite sample before (a) and after (b) experiments. Color version is available online from https://doi.org/10.2465/jmps.181107b.

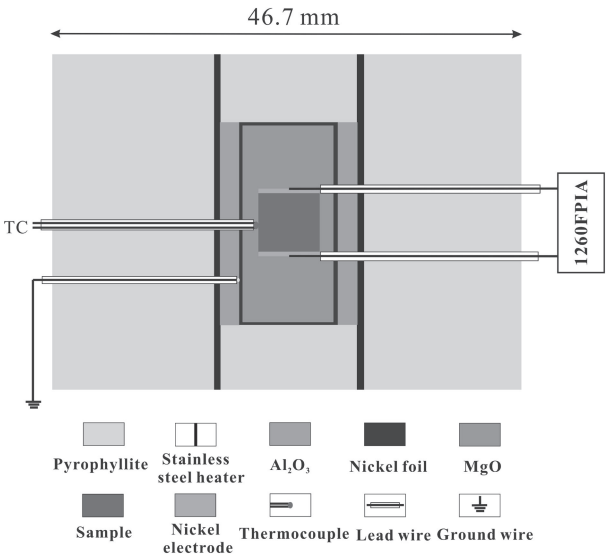

Figure 3. Experimental setup for electrical conductivity measurements at high temperatures and pressures. Color version is available online from https://doi.org/10.2465/jmps.181107b.

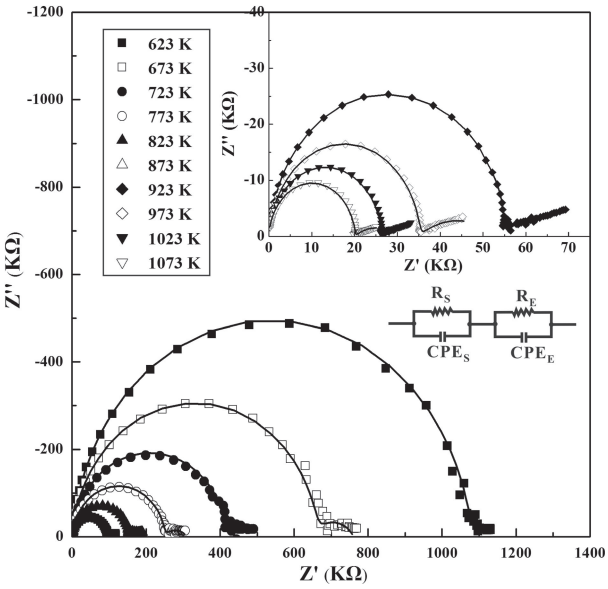

Figure 4. Representative complex impedance spectra for run DS17 granulite at 2.0 GPa and 623–1073 K.

$$\sigma = L / SR \quad (1),$$

where L is the sample height (m), S is the electrode cross-sectional area (m^2), R is the fitting resistance (Ω), and σ is the electrical conductivity of the sample (S/m).

The logarithmic electrical conductivities of the granulite samples were plotted against the reciprocal temperatures at 623–1073 K and 1.0–3.0 GPa. The electrical conductivities of the granulite sample with W_B = 5.49 wt% were measured in two sequential heating and cooling cycles at 2.0 GPa (Fig. 5). After the first heating cycle, the electrical conductivities of the granulite sample measured at the same temperature in different cycles were close to each other, which indicates that the granulite sample remained under steady state after the first heating cycle, and our experimental data were reproducible. For the sample with W_B = 5.49 wt%, two different linear relations between logarithmic electrical conductivity and reciprocal temperature separated by an inflection point were observed. For samples with W_B = 8.75 and 14.79 wt%, the logarithmic electrical conductivity and reciprocal temperature displayed linear relationships under the experimental conditions. As shown in Figure 6, the electrical conductivities of the samples decreased with an increasing pressure, and the effect of pressure on conductivity was weaker than that of temperature. In addition, the electrical conductivities of the granulite samples increased with iron content (Fig. 7). As the sole iron-bearing mineral of the granulite samples, biotite had a marked influence on the sample conductivities. Correspondingly, the sample conductivities increased with biotite content. Unexpectedly, there was no direct correlation between the calcium- and alkali-ion content and the conductivities of the granulite samples (Fig. 7 and Table 2). The conductivities of the granulite samples did not change regularly with the feldspar content (Fig. 7 and Table 1). In a certain temperature range, the relationship between electrical conductivity and temperature fitted the Arrhenius formula:

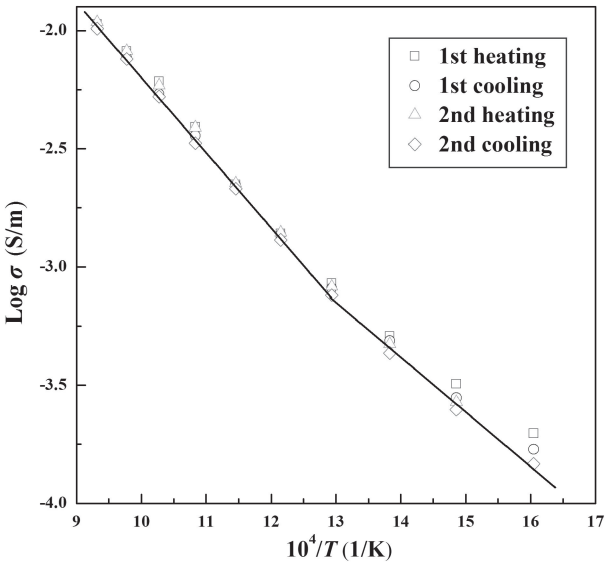

Figure 5. Logarithm of electrical conductivity versus reciprocal temperature for run DS17 granulite during two heating/cooling cycles at 2.0 GPa. Color version is available online from https://doi.org/10.2465/jmps.181107b.

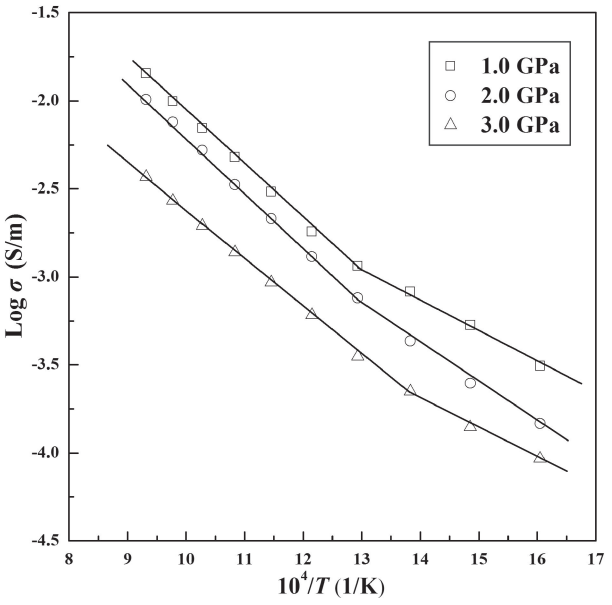

Figure 6. Logarithm of electrical conductivity versus reciprocal temperature for run DS17 granulite at 1.0–3.0 GPa and 623–1073 K.

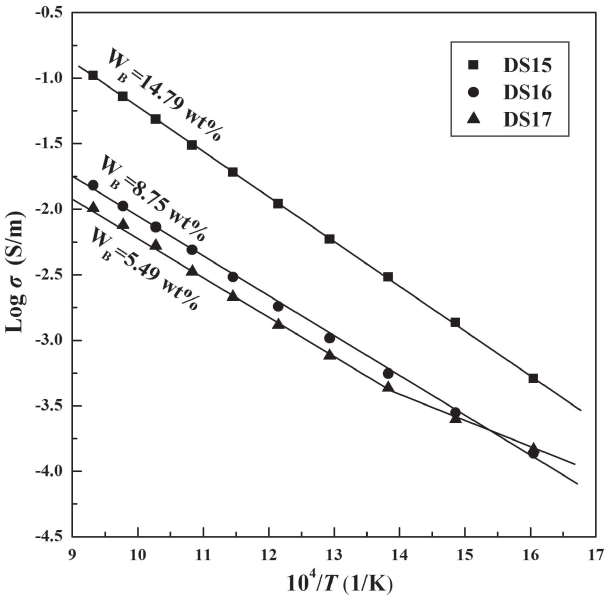

Figure 7. Logarithm of electrical conductivity versus reciprocal temperature for granulite samples with various chemical compositions at 2.0 GPa and 623–1073 K.

$$\sigma = \sigma_0 \exp(-\Delta H / kT) \quad (2),$$

where σ_0 is the pre-exponential factor (K·S/m), k is the Boltzmann constant (eV/K), T is the absolute temperature (K), and ΔH is the activation enthalpy (eV). All fitting parameters for the electrical conductivities of the three granulite samples are listed in Table 3. For the granulite samples with W_B = 8.75 and 14.79 wt%, ΔH was 0.61–0.68 eV at high temperatures and pressures. For the granulite sample with W_B = 5.49 wt%, ΔH was 0.36–0.42 eV in the low-temperature region and 0.55–0.63 eV in the high-temperature region.

DISCUSSION

Influence of Pressure and Chemical Compositions on Electrical Conductivity

The influence of pressure on the electrical conductivities of granulite was much weaker than that of the temperature, and the granulite conductivities decreased slightly with an increase in pressure, which agrees with the influence of pressure on the electrical conductivities of most silicate minerals and rocks (Hu et al., 2011; Dai et al., 2014; Dai and Karato, 2014). At a certain temperature, the granulite conductivities decreased by 0.5 orders of magnitude from 1.0 GPa to 3.0 GPa. The relationship between the electrical conductivities of the main rock-forming minerals (feldspar and quartz) of the granulite and pressure has been investigated in previous studies (Hu et al., 2011; Wang et al., 2012; Hu et al., 2014;). At 1.0–3.0 GPa and 773–1073 K, the electrical conductivities of albite and synthetic anorthite decrease slightly with an increase in pressure (Hu et al., 2011, 2014). For quartz, the electrical conductivities remained almost unchanged with an increase in pressure (Wang et al., 2010). At 1.0 GPa and 473–1173 K, Li et al. (2016) in situ measured the electrical conductivities of phlogopite, which is a special iron-bearing mica. However, the influence of pressure on the biotite conductivities has not been studied.

The chemical compositions of the granulites are very complicated (Table 2), and the content of some compositions must dominate the granulite conductivities. For granulite, the electrical conductivities significantly increased with biotite content (Fig. 7 and Table 1). In addition, the granulite sample conductivities were lower than those of biotite, but higher than those of feldspars and quartz (Fig. 7). The changes in granulite sample conductivities did not correlate with the feldspar and quartz content (Fig. 7 and Table 1). There was no direct correlation between the calcium- and alkali-ion content and the granulite sample conductivities (Fig. 7 and Table 2). This result indicates that the granulite sample conductivities were not dominated by feldspar or quartz at high temperatures and pressures. Therefore, biotite was the dominant mineral that affected the electrical properties of the granulite samples. Biotite was the sole iron-bearing hydrous mineral in the granulite samples. As shown in Figure 2, the IR absorbance of biotite was much higher

Table 3. Fitted parameters of the Arrhenius relation for the electrical conductivity of granulite samples

Run No.	P (GPa)	T (K)	Log σ_0 (S/m)	ΔH (eV)	γ^2
DS15	2.0	623-1073	2.19±0.01	0.68±0.01	0.9999
DS16	2.0	623-1073	1.01±0.05	0.61±0.01	0.9985
DS17	1.0	623-773	-0.56±0.07	0.36±0.01	0.9978
		823-1073	1.08±0.03	0.62±0.01	0.9995
	2.0	623-723	-0.46±0.18	0.42±0.02	0.9937
		773-1073	0.99±0.04	0.63±0.01	0.9992
	3.0	623-723	-1.16±0.14	0.36±0.02	0.9948
		773-1073	0.17±0.02	0.55±0.01	0.9997

than that of feldspar and quartz before and after dehydration, which indicates that biotite was the dominant hydrous mineral in the granulites. The water in biotite remained almost unchanged before and after electrical measurement. In addition, the conductivities of the granulite samples did not increase abruptly with an increase in temperature, and the dehydration temperature of the iron-bearing hydrous mica exceeded 1085 K (Wu et al., 1995). Therefore, the granulite did not experience dehydration at 1.0–3.0 GPa and 673–1073 K. Small polaron conduction was proposed as the conduction mechanism for biotite (Tolland, 1973; Laštovičková, 1991; Rüscher, 2012), and thus the iron content significantly affected the biotite conductivities. Since biotite was the dominant mineral in the samples, the iron content has a remarkable influence on the conductivity of granulite.

Comparison with Previous Studies

The mineralogical assemblage and structure of the natural granulite samples was complicated, and thus we considered each rock sample as a complex whole to analyze the electrical conductivities of the granulite samples with various chemical compositions at high temperature and pressure. As shown in Figure 5, the electrical conductivities of the granulite sample showed good repeatability after the first heating cycle, which indicates that the granulite sample remained stable after the first heating cycle.

At 2.0 GPa and 623–973 K, the electrical conductivities of the granulite samples with various chemical compositions were ~ 10^{-4}–10^{-1} S/m. As important rock-forming minerals, feldspar, biotite, and quartz affect the granulite sample conductivities at high temperature and pressure to varying degrees. Research on the electrical conductivities of the dominant minerals in the granulite samples is significant. Hu et al. (2013) researched the conductivities of alkali feldspar solid solutions at 1.0 GPa and 873–1173 K. They suggested that K^+ and Na^+ are the charge carriers in K-feldspar and albite, respectively. Figure 8 shows that the electrical conductivities of the granulite samples are much higher than those of the alkali feldspars. This result implies that the granulite conductivities were not dominated by feldspars. Wang et al. (2010) researched the conductivities of synthetic quartz at

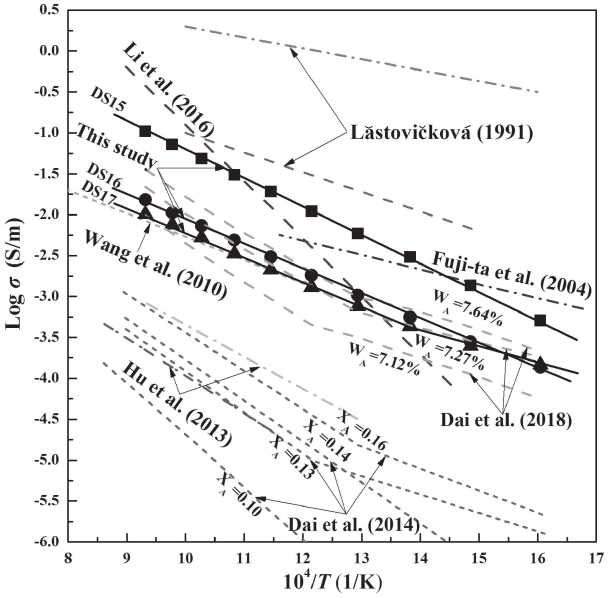

Figure 8. Comparisons of the electrical conductivities of the granulite samples measured at 2.0 GPa in this study with the data measured for other relevant minerals and rocks in previous studies. The dashed pink and dark green lines represent the electrical conductivities of biotite measured in air and argon, respectively (Laštovičková, 1991), the dashed green lines represent the electrical conductivities of gneiss samples with various chemical compositions at 1.5 GPa (Dai et al., 2018), the dashed red lines represent the electrical conductivities of granite samples with various chemical compositions at 0.5 GPa (Dai et al., 2014), the dashed blue line represents the electrical conductivities of granulite at 1.0 GPa (Fuji-ta et al., 2004), the dashed light blue and violet lines represent the electrical conductivities of albite and K-feldspar at 1.0 GPa (Hu et al., 2013), respectively, the dashed brown line represents the electrical conductivities of phlogopite at 1.0 GPa (Li et al., 2016), and the dashed orange line represents the electrical conductivities of quartz at 1.0 GPa (Wang et al., 2010). Color version is available online from https://doi.org/10.2465/jmps.181107b.

850–1600 K and 1.0 GPa. The quartz conductivities were lower than those of the granulite samples, and thus quartz was not the dominant mineral for the granulite conductivities. Laštovičková (1991) investigated the conductivities of biotite using the direct-current method at atmospheric pressure and 293–1473 K. Electrical conductivities measured in air were 1.5 orders of magnitude higher than those measured in argon. A large amount of Fe^{2+} was oxidized to Fe^{3+} in the biotite sample measured in air (Laštovičková, 1991). The conductivities of biotite measured in argon were moderately higher than those of DS15 with plenty of biotites (volume percent: 30%), and much higher than those of DS16 and DS17 with a relatively small quantity of biotite (volume percent: 13% and 20%, respectively). It is proposed that biotite was the dominant mineral for the electrical conductivities of the granulite samples. Compared with another iron-bearing mica, phlogopite, the conductivities of the granulite sample with W_B = 14.79 wt% were lower than those of phlogopite at higher temperatures (above 923 K), and higher than those of phlogopite at lower temperatures (below 923 K). The slope of the linear relation between the logarithmic electrical conductivity of the phlogopite sample and reciprocal temperature was much higher than the slopes observed for the granulite samples (Li et al., 2016). Furthermore, previous studies have researched the electrical conductivities of some rocks with similar mineralogical assemblages of granulite samples. Dai et al. (2014) investigated the electrical conductivities of natural granite samples at 0.5–1.5 GPa and 623–1173 K. The main rock-forming minerals of the granite samples were also quartz, feldspar, and biotite. However, the electrical conductivities of granite were much lower than those of granulite (Fig. 8) because the biotite content of granite was much lower than that of granulite. Dai et al. (2018) studied the electrical conductivities of the gneiss samples with various chemical compositions at 0.5–2.0 GPa and 623–1073 K. As shown in Figure 8, the electrical conductivities of gneiss samples with W_A = 7.27 and 7.64 wt% were close to those of DS15 and DS16, and much lower than those of DS17. In addition, the conductivities of the gneiss sample with W_A = 7.12 wt% were lower than those of the three granulite samples. Fuji-ta et al. (2004) investigated the conductivities of granulite under middle-low crustal pressure and temperature conditions. The conductivities of our granulite samples with W_B = 5.49 and 8.75 wt% at 2.0 GPa were lower than those for the granulite of Fuji-ta et al. (2004). The conductivities of our granulite sample with W_B = 14.79 wt% at 2.0 GPa were slightly higher than those for the granulite of Fuji-ta et al. (2004). This may be caused by the difference in chemical compositions of the granulite samples.

Conduction Mechanism

Conduction mechanisms for silicate minerals and rocks can be determined based on the chemical compositions and thermodynamic parameters (e.g., ΔH). A dominant conduction mechanism tends to exist for a sample when the logarithmic electrical conductivities and reciprocal temperatures conform to a linear relationship in a certain temperature range (Wang et al., 2012; Dai et al., 2014, 2016; Li et al., 2016). For granulite samples with a high iron content (W_B = 8.75 and 14.79 wt%), the logarithmic electrical conductivities and reciprocal temperatures conformed to linear relationships under the experimental conditions. For the granulite sample with a low iron content (W_B = 5.49 wt%), the logarithmic electrical conductivities and reciprocal temperatures exhibited different linear relationships at higher and lower temperatures. This implies that one conduction mechanism dominates the conductivities of granulite samples with a high iron content, and the dominant conduction mechanism for the granulite sample with a low iron content at lower temperature is different from that at a higher temperature.

The complicated mineralogical assemblage and chemical compositions of the samples makes it difficult to determine their conduction mechanisms. Biotite is a hydrous mineral with a high iron content, and feldspar contains abundant alkali ions. Therefore, possible conduction mechanisms for the granulite samples include ionic conduction, hydrogen-related defect conduction, and small polaron conduction. The electrical conductivities of the granulite samples did not correlate with changes in content of calcium and alkali ions (Fig. 7 and Table 2). ΔH for the granulite samples were smaller than those for minerals (feldspars and phlogopite) and rocks (granite and gneiss) that displayed ionic conduction (Hu et al., 2013; Dai et al., 2014; Li et al., 2016; Dai et al., 2018). This result indicates that the calcium and alkali ions were not the main charge carriers in the granulite samples. Previous studies have proposed that hydrogen-related defect or small polaron conduction is the dominant conduction mechanism for many iron-bearing hydrous minerals and rocks, e.g., talc, chlorite, mudstone, epidote, phyllite, amphibole-bearing rocks, and serpentine (Zhu et al., 1999; Guo et al., 2011; Wang et al., 2012; Manthilake et al., 2016; Hu et al., 2017; Sun et al., 2017a, 2017b; Wang et al., 2017). ΔH for iron-bearing hydrous minerals and rocks with hydrogen-related conduction is ~ 0.60–0.80 eV (Guo et al., 2011; Hu et al., 2017), and ~ 0.55–0.80 eV for iron-bearing hydrous minerals and rocks with a small polaron conduction (Wang et al., 2012; Manthilake et al., 2016; Sun et al., 2017b). ΔH for the granulite samples with W_B = 8.75 and

14.79 wt% were 0.61 and 0.68 eV, respectively, and those for the granulite sample with W_B = 5.49 wt% at high temperatures were 0.55–0.63 eV. Therefore, granulite samples with W_B = 8.75 and 14.79 wt% under the experimental conditions and W_B = 5.49 wt% at high temperature exhibited ΔH values that are consistent with those of iron-bearing hydrous minerals and rocks. As an iron-bearing hydrous mineral, biotite was the dominant mineral for the granulite sample conductivities. Previous studies have confirmed that small polaron conduction was the conduction mechanism for biotite (Tolland, 1973; Laštovičková, 1991; Rüscher, 2012). Therefore, small polaron conduction was proposed as the conduction mechanism for granulite samples with W_B = 8.75 and 14.79 wt% under the experimental conditions, and the granulite sample with W_B = 5.49 wt% at high temperatures. For the granulite sample with W_B = 5.49 wt% at low temperatures, the activation enthalpies (0.36–0.42 eV) were close to those of the granites (0.5 eV) at low temperatures. The mineralogical assemblage of the granulite sample with W_B = 5.49 wt% was close to that of the granite (Dai et al., 2014). Therefore, the conduction mechanism for the granulite sample with W_B = 5.49 wt% at low temperatures was proposed to be impurity conduction.

GEOPHYSICAL IMPLICATIONS

Granulite is distributed widely in regional metamorphic belts, where it coexists with other regional metamorphic rocks such as gneiss and schist (Naidu et al., 2011; Patro et al., 2014; Santosh et al., 2015; Takamura et al., 2016; Bhowmik et al., 2018). Therefore, it is significant to research the material compositions and thermodynamic states under the regional metamorphic belts based on the MT data and electrical conductivities of granulites. The SGT is a significant regional metamorphic belt on a global scale. Patro et al. (2014) evaluated the crustal and upper mantle lithospheric electrical structure of the SGT in India using MT data. Under the SGT, four high-conductivity geological bodies are distributed in the crust and are separated by the individual highly resistive geological bodies. The conductivities of the high-conductivity geological bodies were ~ $10^{-1.5}$ S/m at depths of 25–39 km. In addition, the high-conductivity geological bodies are correlated closely in space with the share zones, and thus were proposed to be linked closely to the subduction and collision tectonic processes in the SGT (Patro et al., 2014).

Although the electrical structures of the SGT have been evaluated, the material compositions of the high-conductivity geological bodies have not been researched. Because the SGT is a complicated tectonic unit, the interior of the SGT must contain various materials. The material composition of the Earth's interior can be investigated by combining laboratory data for electrical conductivities with MT results. To this end, it is significant to convert the conductivity–temperature data into conductivity–depth data. According to the thermal model in southern India (Behera, 2011), the electrical conductivities of granulites in this study, gneiss (Dai et al., 2018), granulite (Fuji-ta et al., 2004), and a plagioclase–NaCl–water system (Li et al., 2018) were correlated with depth in southern India. As shown in Figure 9, the electrical conductivities at depths of 0–60 km in southern India are ~ 10^{-3}–$10^{-1.5}$ S/m (Patro et al., 2014). The conductivities of the granulite samples with low iron contents (5.49 and 8.75 wt%) were close to those of Dai et al. (2018) and Fuji-ta

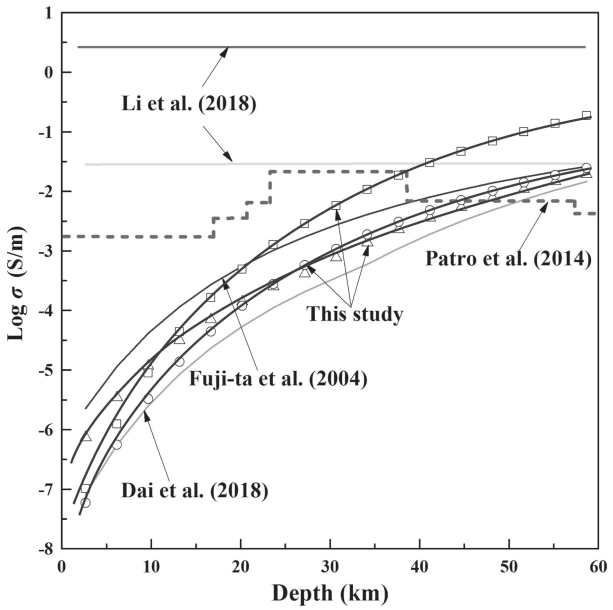

Figure 9. Laboratory-based conductivity–depth profiles constructed from data obtained for our granulite samples in this study, natural gneiss (Dai et al., 2018), natural granulite (Fuji-ta et al., 2004), and synthesized plagioclase–NaCl–H_2O system (Li et al., 2018) based on the thermal structure in southern India (Behera, 2011), and comparison with geophysically inferred field results from southern India. The black solid lines represent the conductivity–depth profiles obtained based on the conductivities of the samples presented in Figure 7 and the thermal structure in southern India. The orange solid line represents the conductivity–depth profiles determined based on the conductivities of gneiss (Dai et al., 2018), the blue solid line represents the conductivity–depth profiles calculated based on the conductivities of granulite (Fuji-ta et al., 2004), and the brown and light blue solid lines represent the electrical conductivities of plagioclase–NaCl–H_2O systems with 24.8 wt% and 9.7 wt% NaCl, respectively (Li et al., 2018). The dashed red line represents the electrical conductivities of HCLs under southern India (Patro et al., 2014). Color version is available online from https://doi.org/10.2465/jmps.181107b.

et al. (2004). For the shallow crust in southern India, the electrical conductivities were higher than the conductivities of metamorphic rocks (granulite and gneiss) and lower than those of the plagioclase–NaCl–water system with 9.7 wt% NaCl, which indicates that a certain quantity of saline fluid may be distributed in the shallow crust in southern India. At depths of 25–39 km, the highest electrical conductivity ($10^{-1.5}$ S/m) of the high-conductivity geological bodies under the ductile shear zones in southern India was higher than that of metamorphic rocks with low iron contents (5.49 and 8.75 wt%) and close to that of the plagioclase–NaCl–water system with 9.7 wt% NaCl. The conductivities of the granulite sample with a high iron content (14.79 wt%) were very close to that at a depth of 39 km and slightly lower than those at shallower depths under the ductile shear zones in southern India. These results indicate that the presence of granulite (main minerals: plagioclase, quartz and biotite) with a high iron content (>14.79 wt%) or saline fluid-bearing rock can be used to interpret the high-conductivity anomalies observed under the ductile shear zones in southern India. Based on the thermal model of Behera (2011), the temperatures at depths of 25–39 km in southern India are 473–923 K, and thus melts cannot form at this depth range (Gaillard, 2005).

CONCLUSIONS

The electrical conductivities of granulite samples significantly increased with an increasing temperature and slightly decreased with an increasing pressure. The iron content markedly enhances the granulite sample conductivities. Granulite with a low iron content exhibited two different conduction mechanisms: impurity conduction at low temperatures and small polaron conduction at high temperatures. For granulite with a high iron content, the proposed conduction mechanism was small polaron conduction under the experimental conditions of 1.0–3.0 GPa and 623–1073 K. Furthermore, the high conductivity anomalies detected under the ductile shear zones in southern India are possibly caused by the presence of granulite (main minerals: plagioclase, quartz, and biotite) with a high iron content (>14.79 wt%) or saline fluid-bearing rock.

ACKNOWLEDGMENTS

This research was financially supported by the Strategic Priority Research Program (B) of the Chinese Academy of Sciences (XDB 18010401), Key Research Program of Frontier Sciences of CAS (QYZDB-SSW-DQC009), “135” Program of the Institute of Geochemistry of CAS, Hundred Talents Program of CAS and NSF of China (41474078, 41774099 and 41772042).

SUPPLEMENTARY MATERIALS

Color versions of Figures 1, 2, 3, 5, 8, and 9 are available online from https://doi.org/10.2465/jmps.181107b.

REFERENCES

Behera, L. (2011) Crustal tomographic imaging and geodynamic implications toward south of Southern Granulite Terrain (SGT), India. Earth and Planetary Science Letters, 309, 166–178.

Bhowmik, S.K., Dasgupta, S., Baruah, S. and Kalita, D. (2018) Thermal history of a Late Mesoproterozoic paired metamorphic belt (?) during Rodinia assembly: New insight from medium-pressure granulites from the Aravalli–Delhi Mobile Belt, Northwestern India. Geoscience Frontiers, 9, 335–354.

Chen, S.B., Guo, X.Z., Yoshino, T., Jin, Z.M. and Li, P. (2018) Dehydration of phengite inferred by electrical conductivity measurements: Implication for the high conductivity anomalies relevant to the subduction zones. Geology, 46, 11–14.

Collins, A.S., Clark, C. and Plavsa, D. (2014) Peninsular India in Gondwana: The tectonothermal evolution of the Southern Granulite Terrain and its Gondwanan counterparts. Gondwana Research, 25, 190–203.

Dai, L.D., Li, H.P., Hu, H.Y. and Shan, S.M. (2009) Novel technique to control oxygen fugacity during high-pressure measurements of grain boundary conductivities of rocks. Review of Scientific Instruments, 80, 033903, https://doi.org/10.1063/1.3097882.

Dai, L.D. and Karato, S. (2014) Influence of FeO and H on the electrical conductivity of olivine. Physics of the Earth and Planetary Interiors, 237, 73–79.

Dai, L.D., Hu, H.Y., Li, H.P., Jiang, J.J. and Hui, K.S. (2014) Influence of temperature, pressure, and chemical composition on the electrical conductivity of granite. American Mineralogist, 99, 1420–1428.

Dai, L.D., Hu, H.Y., Li, H.P., Wu, L., Hui, K.S., Jiang, J.J. and Sun, W.Q. (2016) Influence of temperature, pressure, and oxygen fugacity on the electrical conductivity of dry eclogite, and geophysical implications. Geochemistry, Geophysics, Geosystems, 17, 2394–2407.

Dai, L.D., Sun, W.Q., Li, H.P., Hu, H.Y., Wu, L. and Jiang, J.J. (2018) Effect of chemical composition on the electrical conductivity of gneiss at high temperatures and pressures. Solid Earth, 9, 233–245.

Faul, U.H., Cline, C.J., Andrew, B., Jackson, I. and Garapić, G. (2018) Constraints on oxygen fugacity within metal capsules. Physics and Chemistry of Minerals, 45, 497–509.

Fuji-ta, K., Katsura, T. and Tainosho, Y. (2004) Electrical conductivity measurement of granulite under mid- to lower crustal pressure-temperature conditions. Geophysical Journal International, 157, 79–86.

Fuji-ta, K., Katsura, T., Matsuzaki, T. and Ichiki, M. (2007) Electrical conductivity measurements of brucite under crustal pressure and temperature conditions. Earth Planets and Space, 59, 645–648.

Gaillard, F. (2005) Electrical conductivity of magma in the course of crystallization controlled by their residual liquid composi-

tion. Journal of Geophysical Research: Solid Earth, 110, B06204, https://doi.org/10.1029/2004JB003282.

Guo, X.Z., Yoshino, T. and Katayama, I. (2011) Electrical conductivity anisotropy of deformed talc rocks and serpentinites at 3 GPa. Physics of the Earth and Planetary Interiors, 188, 60–81.

Hu, H.Y., Li, H.P., Dai, L.D., Shan, S.M. and Zhu, C.M. (2011). Electrical conductivity of albite at high temperatures and high pressures. American Mineralogist, 96, 1821–1827.

Hu, H.Y., Li, H.P., Dai, L.D., Shan, S.M. and Zhu, C.M. (2013) Electrical conductivity of alkali feldspar solid solutions at high temperatures and high pressures. Physics and Chemistry of Minerals, 40, 51–62.

Hu, H.Y., Dai, L.D., Li, H.P., Jiang, J.J. and Hui, K.S. (2014) Electrical conductivity of K–feldspar at high temperature and high pressure. Mineralogy and Petrology, 108, 609–618.

Hu, H.Y., Dai, L.D., Li, H.P., Hui, K.S. and Sun, W.Q. (2017) Influence of dehydration on the electrical conductivity of epidote and implications for high conductivity anomalies in subduction zones. Journal of Geophysical Research: Solid Earth, 122, 2751–2762.

Hu, H.Y., Dai, L.D., Li, H.P., Sun, W.Q. and Li, B.S. (2018) Effect of dehydrogenation on the electrical conductivity of Fe–bearing amphibole: Implications for high conductivity anomalies in subduction zones and continental crust. Earth and Planetary Science Letters, 498, 27–37.

Hui, K.S., Zhang, H., Li, H.P., Dai, L.D., Hu, H.Y., Jiang, J.J. and Sun, W.Q. (2015) Experimental study on the electrical conductivity of quartz andesite at high temperature and high pressure: evidence of grain boundary transport. Solid Earth, 6, 1037–1043.

Laštovičková, M. (1991) Laboratory measurements of electrical conductivity of biotites. Studia Geophysica Et Geodaetica, 35, 125–129.

Li, Y., Yang, X.Z., Yu, J.H. and Cai, Y.F. (2016) Unusually high electrical conductivity of phlogopite: the possible role of fluorine and geophysical implications. Contributions to Mineralogy and Petrology, 171, 1–11.

Li, Y., Jiang, H.T. and Yang, X.Z. (2017) Fluorine follows water: Effect on electrical conductivity of silicate minerals by experimental constraints from phlogopite. Geochimica et Cosmochimica Acta, 217,16–27.

Li, P., Guo, X., Chen, S., Wang, C., Yang, L. and Zhou, X. (2018) Electrical conductivity of the plagioclase–NaCl–water system and its implication for the high conductivity anomalies in the mid–lower crust of Tibet Plateau. Contributions to Mineralogy and Petrology, 173, 16, https://doi.org/10.1007/s00410–018–1442–9.

Manthilake, G., Mookherjee, M., Bolfan–Casanova, N. and Andrault, D. (2015) Electrical conductivity of lawsonite and dehydrating fluids at high pressures and temperatures. Geophysical Research Letters, 42, 7398–7405.

Manthilake, G., Bolfan–Casanova, N., Novella, D., Mookherjee, M. and Andrault, D. (2016) Dehydration of chlorite explains anomalously high electrical conductivity in the mantle wedges. Science Advances, 2, e1501631, https://doi.org/10.1126/sciadv.1501631.

Mathez, E.A., Duba, A.G., Peach, C.L., Leger, A., Shankland, T.J. and Plafker, G., (1995) Electrical–conductivity and carbon in metamorphic rocks of the Yukon–Tanana Terrane, Alaska. Journal of Geophysical Research: Solid Earth, 100, 10187–10196.

Naidu, G.D., Manoj, C., Patro, P.K., Sreedhar, S.V. and Harinarayana, T. (2011) Deep electrical signatures across the Achankovil shear zone, Southern Granulite Terrain inferred from magnetotellurics. Gondwana Research, 20, 405–426.

Patro, P.K., Sarma, S.V.S. and Naganjaneyulu, K. (2014) Three–dimensional lithospheric electrical structure of Southern Granulite Terrain, India and its tectonic implications. Journal of Geophysical Research: Solid Earth, 119, 71–82.

Podoba, R., Stubna, I., Trnovcova, V. and Trnik, A. (2014) Temperature dependence of DC electrical conductivity of kaolin. Journal of Thermal Analysis and Calorimetry, 118, 597–601.

Rüscher, C.H. (2012) Temperature–dependent absorption of biotite: small–polaron hopping and other fundamental electronic excitations. European Journal of Mineralogy, 24, 817–822.

Roberts, J.J. and Tyburczy, J.A. (1991) Frequency dependent electrical properties of polycrystalline olivine compacts. Journal of Geophysical Research: Solid Earth, 96, 16205–16222.

Romo, J.M., Gomez–Trevino, E., Flores–Luna, C. and Garcia–Abdeslem, J. (2017) Electrical conductivity of the crust in central Baja California, Mexico, based on magnetotelluric observations. Journal of South American Earth Sciences, 80, 18–28.

Saltas, V., Chatzistamou, V., Pentari, D., Paris, E., Triantis, D., Fitilis, I. and Vallianatos, F. (2013) Complex electrical conductivity measurements of a KTB amphibolite sample at elevated temperatures. Materials Chemistry and Physics, 139, 169–175.

Santosh, M., Yang, Q.Y., Shaji, E., Tsunogae, T., Ram Mohan, M. and Satyanarayanan, M. (2015) An exotic Mesoarchean microcontinent: the Coorg Block, southern India. Gondwana Research, 27, 165–195.

Sun, W.Q., Dai, L.D., Li, H.P., Hu, H.Y., Wu, L. and Jiang, J.J. (2017a) Electrical conductivity of mudstone before and after dehydration at high temperatures and pressures. American Mineralogist, 102, 2450–2456.

Sun, W.Q., Dai, L.D., Li, H.P., Hu, H.Y., Jiang, J.J. and Hui, K.S. (2017b) Effect of dehydration on the electrical conductivity of phyllite at high temperatures and pressures. Mineralogy and Petrology, 111, 853–863.

Takamura, Y., Tsunagae, T., Santosh, M., Malaviarachchi, S.P.K. and Tsutsumi, Y. (2016) U–Pb geochronology of detrital zircon in metasediments from Sri Lanka: Implications for the regional correlation of Gondwana fragments. Precambrian Research, 284, 434–452.

Tolland, H.G. (1973) Mantle conductivity and electrical properties of garnet, mica and amphibole. Nature Physical Science, 241, 35–36.

Wang, D.J., Li, H.P., Matsuzaki, T. and Yoshino, T. (2010) Anisotropy of synthetic quartz electrical conductivity at high pressure and temperature. Journal of Geophysical Research: Solid Earth, 115, B09211, https://doi.org/10.1029/2009JB006695.

Wang, D.J., Guo, X.Y., Yu, Y.J. and Karato, S. (2012) Electrical conductivity of amphibole–bearing rocks: Influence of dehydration. Contributions to Mineralogy and Petrology, 164, 17–25.

Wang, D.J., Liu, X.W., Liu, T., Shen, K.W., Welch, D.O. and Li, B.S. (2017) Constraints from the dehydration of antigorite on high conductivity anomalies in subduction zones. Scientific Reports, 7, 16893, https://doi.org/10.1038/s41598–017–16883–4.

Wu, Y., Ma, X.X., Zhang, Z.P., Jiao, S.W., Duan, K., Dong, H., Wang, X.W., Ma, T., Li, P.J., Liang, Z.Y., Cao, Y.G., Kong, C.P. and Ma, L. (2016) Geochemical fatures of the Nyainqentanglha Group in the western Lhasa Terrane, western Tibet and their tectonic significance. Acta Geological Sinica, 90,

3081–3098.

Wu, Z.X., Deng, J.F., Wyllie, P.J. and Newman, S. (1995) Dehydration–melting experiment of the biotite–gneiss, eastern Hebei, at 1 GPa pressure. Scientia Geologica Sinica, 30, 12–18.

Xu, Y.S., Shankland, T.J. and Duba, A.G. (2000) Pressure effect on electrical conductivity of mantle olivine. Physics of the Earth and Planetary Interiors, 118, 149–161.

Yang, X.Z., Keppler, H., McCammon, C. and Ni, H.W. (2012) Electrical conductivity of orthopyroxene and plagioclase in the lower crust. Contributions to Mineralogy and Petrology, 163, 33–48.

Zhang, S.G., Zhang, Z.Q., Song, B., Tang, S.H., Zhao, Z.R. and Wang, J.H. (2004) On the existence of neoarchean materials in the douling complex, eastern Qinling–Evidence from U–Pb SHRIMP and Sm–Nd geochronology. Acta Geologica Sinica, 78, 800–806.

Zhou, W.G., Fan, D.W., Liu, Y.G. and Xie, H.S. (2011) Measurements of wave velocity and electrical conductivity of an amphibolite from southwestern margin of the Tarim Basin at pressures to 1.0 GPa and temperatures to 700 °C: comparison with field observations. Geophysical Journal International, 187, 1393–1404.

Zhu, M.X., Xie, H.S., Guo, J., Zhang, Y.M. and Xu, Z.M. (1999) Electrical conductivity measurement of serpentine at high temperature and pressure. Chinese Science Bulletin, 44, 1903–1907.

Manuscript received November 7, 2018
Manuscript accepted March 2, 2019
Published online April 9, 2019
Manuscript handled by Toru Inoue